Neuron, Volume *78*

Supplemental Information

Interactions between a Receptor Tyrosine Phosphatase and a Cell Surface Ligand Regulate Axon Guidance and Glial-Neuronal Communication

Hyung-Kook (Peter) Lee, Amy Cording, Jost Vielmetter, and Kai Zinn

Supplemental Experimental Procedures for the AlphaScreen experiment (Figure S3).

All assays were carried out in 384-well white opaque plates (Whatman, 7701 3100). For the experiment in Figure S3B, 2.5 µl of Sas-Fc (40nM) and 2.5 µl of 10D-AP (40 nM) were mixed together. To create the binding curves of Figure S3A, the amounts of Sas-Fc and 10D-AP were systematically varied, with the maximum amount used being 2.5 µl of a 100 nM stock (see Figure S3 legend). The mixed proteins were incubated for 4 hr at room temperature. 20 µl of a solution containing anti-human IgG coated acceptor beads (PerkinElmer alphaLISA kit, AL205C) diluted to 25 µg/ml in alphaLISA immunoassay buffer (PerkinElmer, AL000C) containing mouse biotin-labeled anti-AP antibody (clone 8B6.18) (Neomarkers, MS-208-B) at 1.65 nM was added, and incubation was continued for 1 hr at room temperature. Subsequently, 25 µl of 80 ug/ml streptavidin coated donor beads (PerkinElmer, AL205C), were added at 25 µg/ml in AlphaLISA immunoassay buffer, and incubation was continued for another 1 hr. at room temperature. The plates were then read on a Synergy 2 (BioTek) multiplate reader at 570 nm and data were collected using Gen5 2.0 software (BioTek). Owing to the light-

sensitivity of the beads, all assay steps were performed under subdued lighting, and the incubation steps were carried out in the dark. The microplate reader was set up and conditions were optimized using AlphaScreen omnibeads, which contain all the chemicals necessary to produce a strong AlphaScreen signal without the presence of an AlphaScreen Acceptor bead (PerkinElmer, 6760626D).

The major purpose of the grid experiment of panel A was to find the concentrations of proteins at which the binding signal would be maximal. To find this maximum, we needed to reach concentrations at which binding in solution outweighs binding of the bead-bound proteins to each other. This should cause the signal to decrease (the 'hook effect'), allowing us to define a peak that represents the maximum signal. However, the graph shows that we were unable to reach high enough concentrations of protein to observe the hook effect, since the signal increased up to the maximum concentrations of proteins used. We could not go up to the next concentration step in the grid (316 nM of each protein), because when stocks of purified Sas-Fc were concentrated to above 120 nM the protein precipitated. As a consequence, we do not know at what concentrations the maximal binding signal might be obtained. It was clear, however, that Sas-Fc::10D-AP interactions did not generate strong AlphaScreen signals at any concentration we were able to attain. We were able to produce 40-fold stronger signals, without an increase in background, for lower concentrations of Dscam-AP and Dscam-Fc. While the results in (A) and (B) shows that Sas-Fc binds selectively to 10D-AP, much better signal-to-background ratios were obtained in the modified ELISA experiment of Figure 3. Because of this, and because the absolute signal values in the AlphaScreen were very low for Sas-Fc::10D-AP relative to Dscam, for reasons we do

not fully understand, we used the ELISA to generate the key binding data in the paper, with multiple replicates and controls.

Supplemental Experimental Procedures for the S2 cell aggregation experiment (Figures 3 and S3).

S2 cells were cotransfected, using Effectene, with 1:20 mixtures of a puromycin resistance plasmid (Iwaki et al., 2003) and metallothionein promoter plasmids containing either full-length Ptp10D (Fashena and Zinn, 1997) or a fusion of the entire XC domain of the large Sas isoform to mCD8-GFP. After 2 days, stably transfected cells were selected with 10 µg/ml puromycin and grown out for 3 days. Expression of Ptp10D and Sas was induced with $CuSO_4$ (700 µM), and cells were incubated for 4 more days. Sodium butyrate (5 mM) was added and cells incubated overnight. Ptp10D and Sas cells were then washed and incubated alone or together at ~10^6 cells/ml in serum-free S2 medium overnight (Siebert et al., 2009), followed by fixation and staining with anti-Ptp10D and anti-Sas.

Note that it is not possible to quantitate these cell aggregation results, because most cells expressing Ptp10D are not involved in clusters and most Ptp10D cell clusters are not associated with Sas cells. Thus, as in the (Siebert et al., 2009) paper on *trans* interactions between Sidestep and Beaten Path, we have simply presented typical data as images.

Supplementary Figure S1

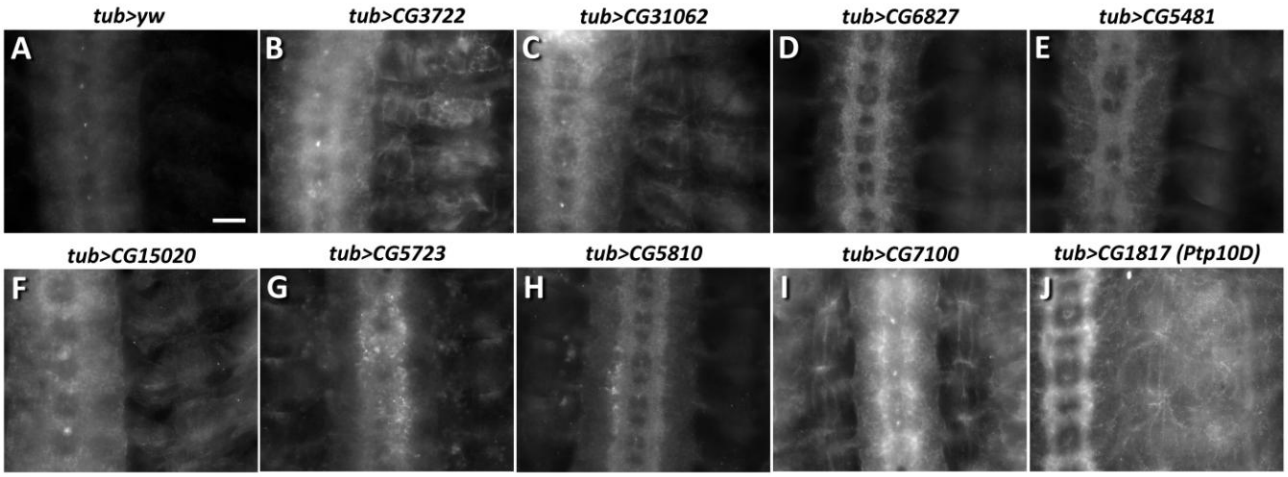

Figure S1 (related to Figure 1). 10D-AP staining of embryos expressing 9 candidate binding partners using tub-GAL4.

Staining was performed as in Figure 1.

(A) tub-GAL4 control. Note that the CNS axon ladder is stained, but there is no staining in the periphery.

(B) tub>CG3722 (E-cadherin/Shotgun). The CNS is brighter than in control, and bright staining in the periphery is observed.

(C) tub>CG31062 (Sidestep). The pattern is similar to (B).

(D) tub>CG6827 (Neurexin IV). The CNS is bright, but peripheral staining is dim.

(E) tub>CG5481 (Robo2/leak). The pattern is similar to (D). Note that the CNS axon ladder is altered by Robo2 overexpression.

(F) tub>CG15020 (a ZP domain protein). The pattern is similar to (C).

(G) tub>CG5723 (Ten-m). The CNS has a bright granular appearance, and muscle attachment sites are prominent.

(H) tub>CG5810 (an LRR protein). The pattern is similar to (D).

(I) tub>CG7100 (Cad-N). The muscle fibers are clearly outlined, and CNS axon staining is very bright.

(J) tub>CG1817 (Ptp10D). Note that axons but not cell bodies are stained in the CNS, consistent with the restriction of endogenous and overexpressed Ptp10D to axons. The muscle fiber outlines are clearly visible.

Scale bar, 20 μm.

Supplementary Figure S2

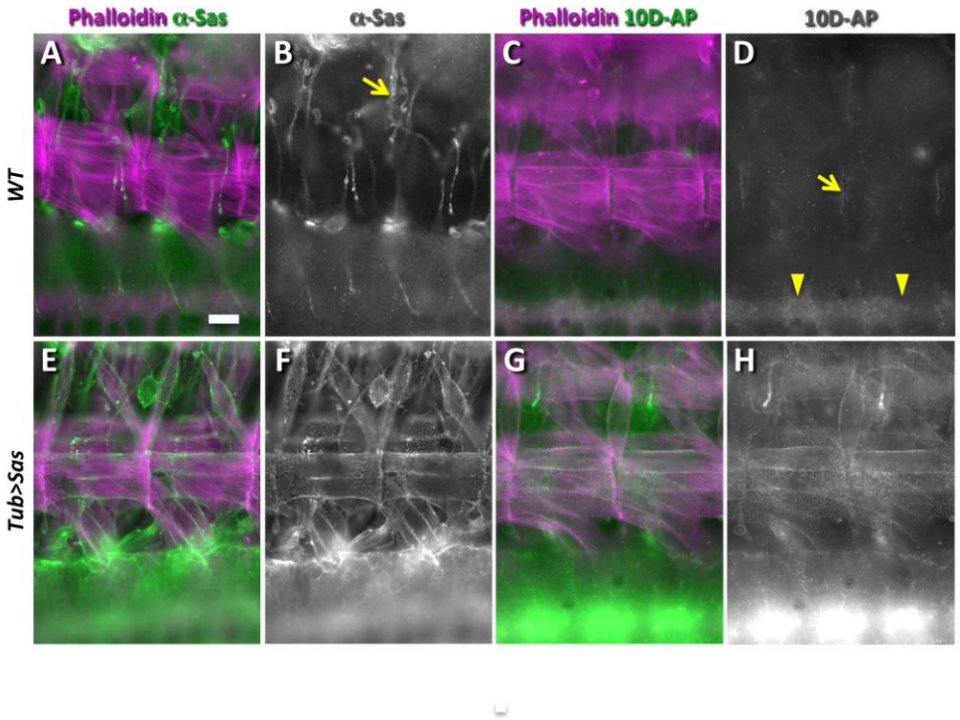

Figure S2 (related to Figures 1 and 2). 10D-AP and anti-Sas label the same patterns in Sas ectopic expression embryos.

Embryos were stained either with anti-Sas or 10D-AP (green/white) plus rhodamine-phalloidin (to visualize muscle fibers; magenta). 10D-AP and anti-Sas cannot be used together because anti-Sas is a rabbit antibody and rabbit anti-AP is used as the secondary antibody to detect 10D-AP. Each image shows the ventral portion of two body wall segments, with anterior to the left and dorsal up. The VNC is at the bottom, and one longitudinal tract is visible in each panel. The muscles in the wild-type images seem slightly smaller because the embryos were less stretched than the Tub>Sas

embryos during dissection. (A, C, E, G) show both signals, while (B, D, F, H) show only the anti-Sas or 10D-AP signal, in white.

(A, B) In wild-type, Sas is expressed on tracheal branches (arrow), but not on muscle fibers. Phalloidin labels muscle fibers and a CNS longitudinal axon tract (out of focus).

(C, D) In wild-type, 10D-AP faintly labels muscle attachment sites (arrow). Staining of the longitudinal tract (out of focus) is visible with phalloidin in (C) and with 10D-AP in (D) (arrowheads).

(E, F) In embryos in which the Sas cDNA construct is driven by tub-GAL4 (Tub>Sas), anti-Sas brightly labels muscle fibers. The longitudinal tract is brighter than in (A), indicating that Sas is expressed at higher levels on axons.

(G, H) In Tub>Sas embryos, 10D-AP labels muscle fibers. This pattern is almost identical to that seen in (E, F). The longitudinal tract is much brighter in (G) and (H) than in (C) and (D), reflecting the higher levels of 10D-AP staining on axons.

Scale bar, 10 μm.

Supplementary Figure S3

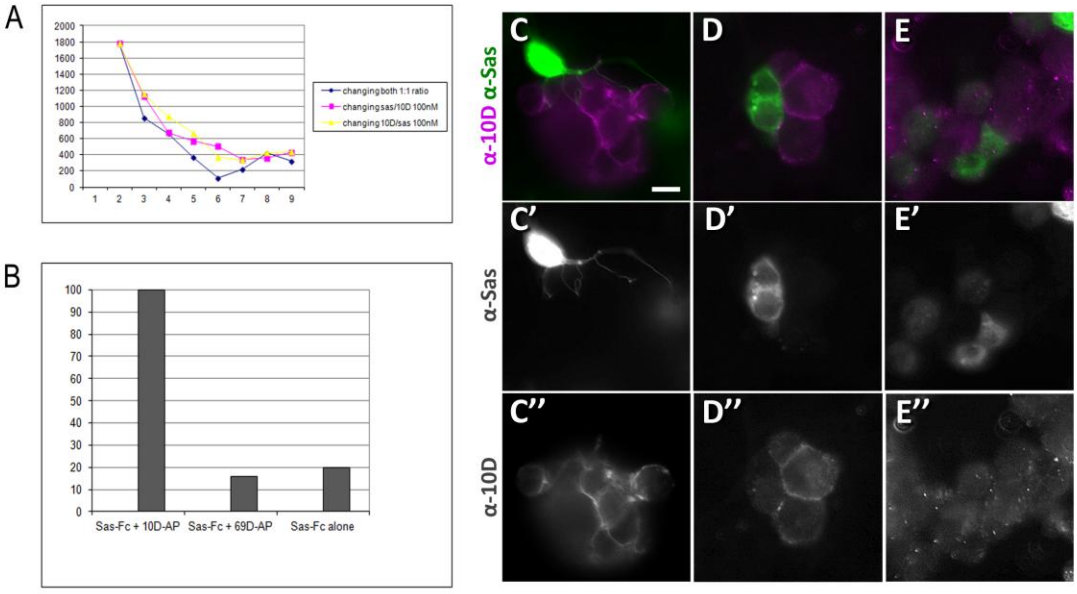

Figure S3 (related to Figure 3). Using the AlphaScreen and S2 cell aggregation to evaluate binding of Ptp10D to Sas.

(A) This graph shows the results of a 'grid' experiment, in which varying concentrations of 10D-AP and Sas-Fc were used for binding. Three sets of half-logarithmic ($10^{0.5}$-fold) dilutions were performed, starting from a 100 nM stock of each protein. For the blue curve, both proteins were diluted; for the yellow curve, Sas-Fc was held at 100 nM and 10D-AP was diluted; for the pink curve, 10D-AP was held at 100 nM and Sas-Fc was diluted. Each point on the *x* axis, starting with point 2, for which both proteins are at 100

nM, represents a dilution step. For the final step (point 9), one or both proteins were brought to zero concentration. The *y* axis is absorbance at 570 nm. The three binding curves all have similar shapes. This experiment shows that Sas-Fc and 10D-AP exhibit concentration-dependent binding to each other (see Supplementary Experimental Procedures for further information).

(B) An example AlphaScreen experiment in which Sas-Fc and 10D-AP were each used at 40 nM. The Sas-Fc::10D-AP signal is set at 100%. In this experiment, as well as in the grid experiment of (A), the signal-to-background ratio is 5- to 6-fold.

(C-E) High magnification views of portions of clusters, showing apposition of Sas and Ptp10D cells.

(C, C', C") A single Sas cell extends processes that intercalate between Ptp10D cells.

(D, D', D") Two Sas cells, which may have recently divided, are apposed to three Ptp10D cells.

(E, E', E") Two bright Sas cells within a cluster of Ptp10D cells. Note the straight borders of the interfaces between the right-hand Sas cell and the Ptp10D cells, which are suggestive of adhesion.

Scale bar, 10 μm.

Supplementary Figure S4

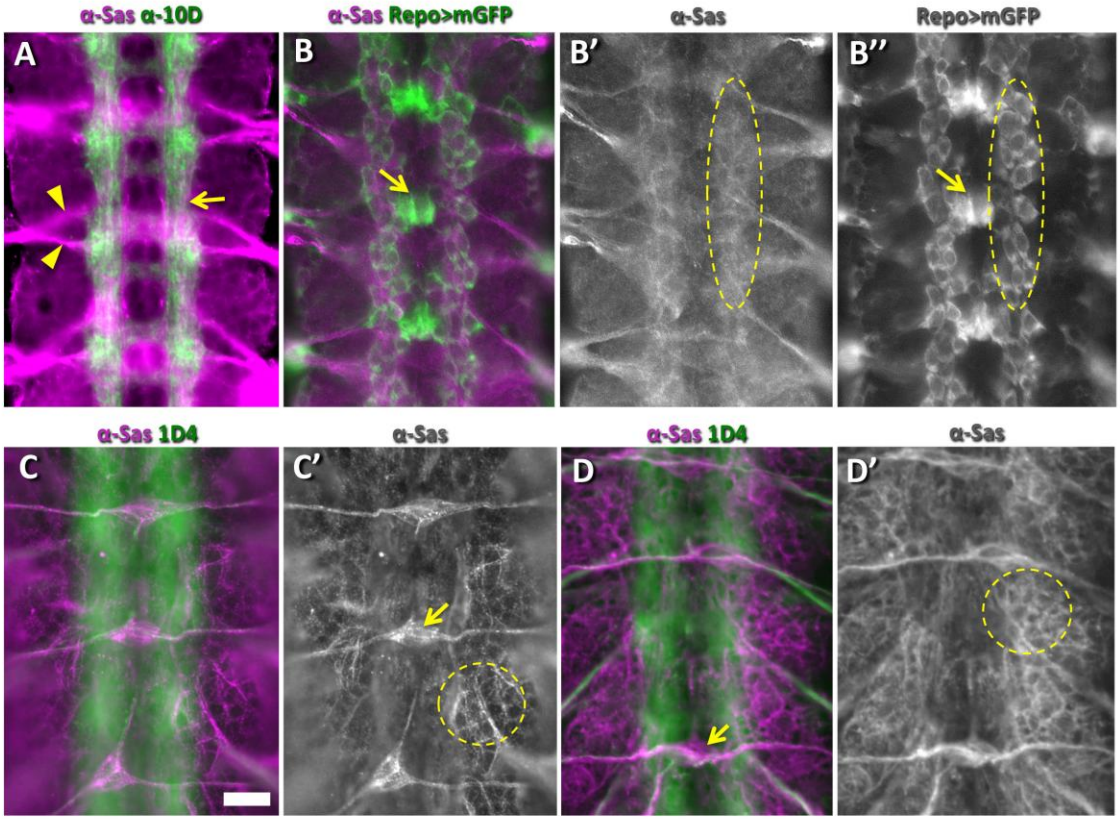

Figure S4 (related to Figure 4). Expression of Sas on CNS glia.

(A) This is a merge of the images in Figures 4A and B, showing the superimposition of Sas (magenta) and Ptp10D (green) expression. A longitudinal tract is indicated (arrow), as are the intersegmental and segmental nerve roots (arrowheads).

(B, B',B") Visualization of Repo-expressing CNS glia in Repo>mCD8-GFP embryos by double-staining with anti-GFP (green/white) and anti-Sas (magenta/white). Note that the longitudinal (interface) glia along the longitudinal tracts (dotted outline) express both GFP and Sas. The channel glia, which are dorsally located at the midline (arrows), do not express Sas, or express it at much lower levels.

(C, C', D, D') These two CNS images, from two different late stage 16 embryos, show anti-Sas (magenta/white) and 1D4 (green/white) staining. The focal planes are very dorsal, so that the 1D4 longitudinal bundles are completely out of focus. The dorsal median (DM) cells (arrow), which are on the dorsal surface of the CNS and express Sas at high levels, serve as points of reference.

(C, C') The focal plane is at the level of the DM cells. In this focal plane, a web of Sas-expressing apical cell surfaces is observed (dotted outline). These are likely to be perineurial and subperineurial glia, which enwrap the cell bodies of the CNS. Perineurial glia do not express Repo.

(D, D') The focal plane is slightly ventral to the DM cells, which are now out of focus. Sas-expressing cells are observed on top of and lateral to the longitudinal tracts (dotted outline). These are likely to be interface glia.

Scale bar, 10 μm.

Supplementary Figure S5

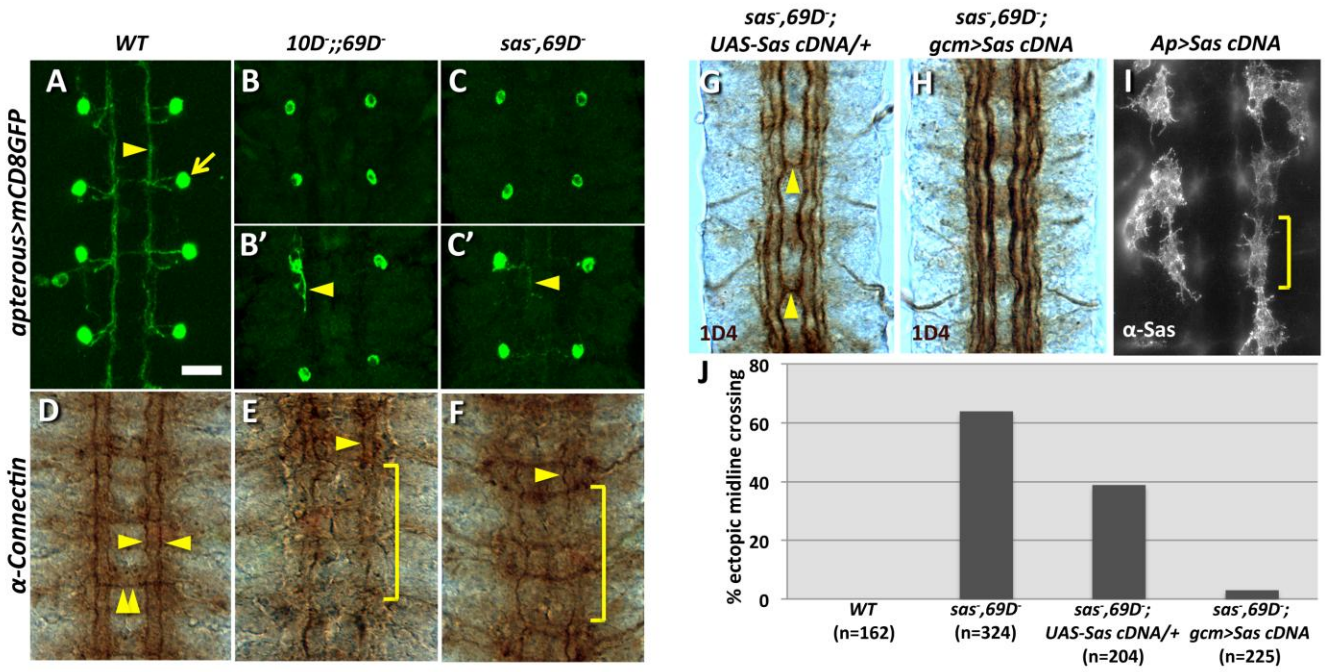

Figure S5 (related to Figure 6). *Ptp10D Ptp69D* and *sas Ptp69D* phenotypes for Apterous (Ap) and Connectin neurons, and rescue of *sas Ptp69D* phenotype by glial expression of Sas.

(A-C) Confocal *z*-stacks of the dorsal region of the VNC, showing one Ap cell body per hemisegment and the longitudinal bundles formed by the Ap axons (arrowhead in (A)). Note that there are several other Ap cell bodies ventral to these cells that also contribute axons to these bundles; these are not visible in these *z*-stacks.

(A) The normal pattern of Ap cell bodies (arrow) and axons in late stage 16 embryos visualized by driving mCD8-GFP with Ap-GAL4. Scale bar, 10 µm.

(B, C) In most *Ptp10D Ptp69D* and *sas Ptp69D* embryo segments, there are no Ap axons. Only the cell bodies are visible, and they express GFP at reduced levels.

(B', C') When Ap axons are observed, they are truncated and extend posteriorly rather than anteriorly (arrows).

(D) In wild-type late stage 16 embryos, anti-Connectin strongly stains two axon bundles (arrowheads) in each longitudinal tract and a commissural bundle (double arrowhead). The longitudinal bundles are ventral to the 1D4 bundles. There is additional weaker staining on many other cell bodies and axons.

(E) In *Ptp10D Ptp69D*, the inner bundle is present (arrowhead), although it has some gaps, but the outer longitudinal bundle is usually missing (bracket). In this genotype, abdominal segments have weaker Connectin staining than thoracic segments (top segment is T3).

(F) A similar phenotype is observed in *sas Ptp69D,* but abdominal segments stain as strongly as thoracic segments.

(G) A *sas Ptp69D/Df, UAS-Sas* embryo stained with 1D4. Two segments with ectopic midline crossing are indicated.

(H) A *sas Ptp69D/Df, Gcm-GAL4, UAS-Sas* embryo. All three longitudinal tracts are present and unbroken, and there are no ectopic midline crossing events.

(I) An embryo overexpressing Sas from the Ap-GAL4 driver, stained with anti-Sas. In this image, the Ap cell bodies (see panel (A) for the mCD8-GFP pattern conferred by this driver) are below the plane of focus. Note that although Sas is overexpressed only by these few cell bodies, anti-Sas reactivity spreads out within a plane dorsal to these cell bodies, presumably in the ECM. The yellow bracket indicates the Sas pattern

associated with Sas overexpression by a single Ap neuron cluster. If all Sas was transmembrane and associated with Ap neuron cell surfaces, one would expect to see a pattern like that in (A). Endogenous Sas is present in this embryo, but is at much lower levels, so is not seen at this exposure.

(J) Bar graph of ectopic midline crossing phenotype. The presence of the UAS-Sas cDNA element reduces the frequency of ectopic midline crossing, suggesting that there is leaky expression from this element in the absence of a driver. When Gcm-GAL4 is also present, there is almost no ectopic midline crossing (3%).

Supplementary Figure S6

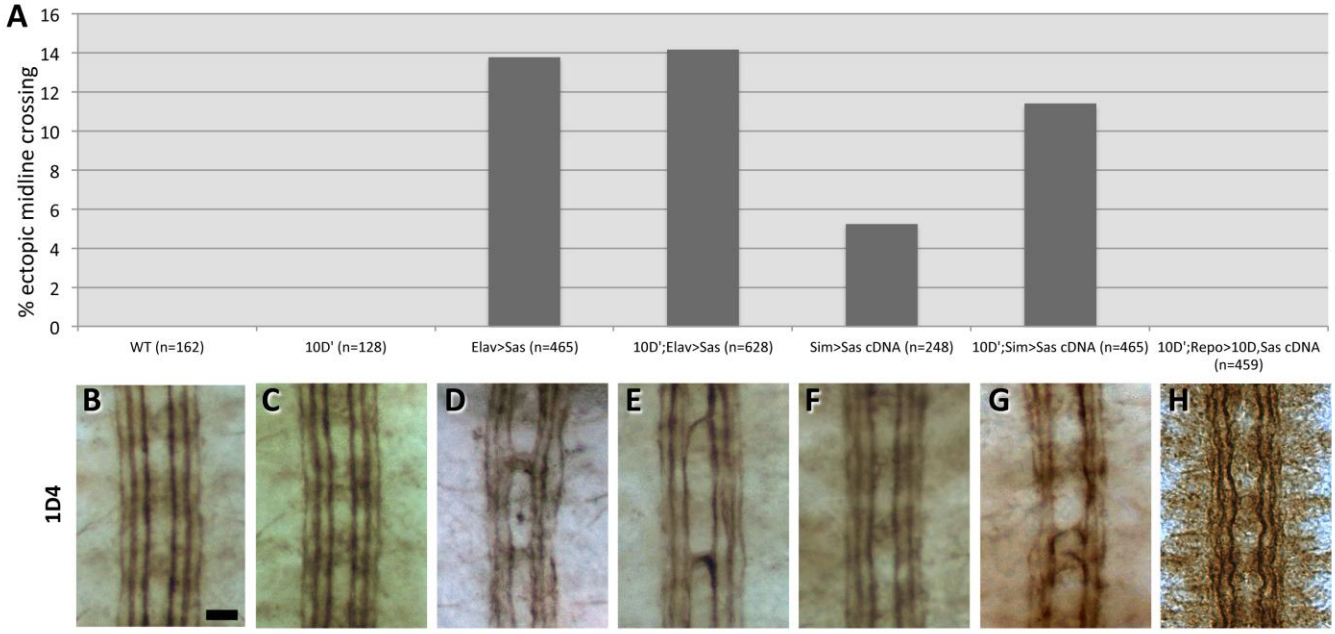

Figure S6 (related to Figure 7). Ectopic midline crossing caused by Sas overexpression in neurons and midline glia, in wild-type and *Ptp10D*-backgrounds.

(A) The CNS has a normal structure when Sas is expressed from the Elav-GAL4 or Sim-GAL4 drivers, but occasional midline crossing of the inner 1D4 bundle is observed. This bar graph shows that the percentage of ectopic midline crossing is not changed when Ptp10D is genetically removed from Elav>Sas embryos, but is doubled when Ptp10D is removed from Sim>Sas embryos. Coexpression of Ptp10D and Sas in *Ptp10D* embryos bearing the Repo-GAL4 driver completely rescues the ectopic midline

crossing phenotype (compare to Figure 7E). The number of segments analyzed is indicated.

(B-H) Representative images (whole-mount embryos) of 1D4 staining of the genotypes shown in (A).

Scale bar, 10 μm.

Table S1.

CG #	Gene name	Line #
CG7749	fat2	GE20158
CG17941	dachsous	GE16163
CG11895	fmi/stan	GS9046
CG10239	Cad96Ca	GE24017
CG4655		GE22560
CG6445		GE22619
CG6977		GE20793
CG31009	Cad99c	d04999
CG31774	friend of echinoid	GE13572
CG3624		GS7500
CG4135	beaten path-IIb	EY07690
CG4814		EY01251
CG32600	dpr8	GE1992
CG5597		GE18518
CG7607		EP3313
CG7644	beaten path-Ib	GS12659
CG10946	dpr14	GS7441
CG31369		GS12277
		GE21731
CG31708		GS10376
		GE15186
CG31431		GE22558
CG33141	sticks and stones	EY08142
CG31646		GE15020
CG14372		EY08788
CG14469	dpr12	f07539
CG31361	dpr17	f07135
CG15009	ImpL2	d11062
CG15312		GS7364
CG15630		GE14234

CG12191	dpr20	GS12770
		GE17036
CG8779	Neuromusculin	GS9446
CG6669	Klingon	GS10439
CG8964		EY03841
CG13506		GE16794
CG14521		EY02750
CG32311	zormin	d08887
CG17716	faint sausage	GS10625
CG7223	heartless	d07110
CG8222	Pvr	f05484
CG8967	off-track	d01360
CG5227	sidekick	EP369
CG5481	robo2	EP2582
CG6490		GE21193
CG9211	iHog	GE16164
CG31190		f00600
CG14964		GS11359
CG15427	turtle	GS9718
CG17800	Dscam	d01097
CG17839		GS11043
CG31738	CG31738	GE13451
CG6173	Kallmann	d01966
		f00379
CG18630		f07661
CG32796	boi	GE4127
CG14226	domeless	d09436
CG6899	Ptp4E	EP425
CG1817	Ptp10D	EP1172
CG2005	PTP99A	EY07423
CG18085	sevenless	GS8057
		GE3589
CG10236	Laminin A	GS10699
		EP3678

CG15288	Laminin A1,2	GS7312
	wing blister	GE14893
CG7123	Laminin B1	GS9163
		GS11222
		EP2178
CG3322	Laminin B2	f01875
CG7981	trol	GE10067
CG3619	Delta	GS3299
CG10521	Netrin B	GS1029
CG8355	Slit	EY10695
CG2991		GE13774
CG3135	shifted	GE946
CG4090		GE13141
CG4250		GE17627
CG5723	ten-m	GS9267
		EY03921
CG5639		f05052
CG8403	SP2353	d01706
CG32179	spitz2(Keren)	GS3237
CG6827	Neurexin IV	EP809
		EP604
CG14307	fruitless	GS3153
CG7447		EY07651
CG7565		GS9380
		GE25495
		EY04273
CG10334	spitz	d03659
CG10491	vein	GS12044
CG11101	pawn	GE10541
CG11326	Thrombospondin	GE10734
CG11377		EY09172
CG17610	gurken	d10614
CG32356	ImpE1	GS10647
		GS11510
		GE23751

CG12781	nahoda	GE16167
		EP627
CG12086	cueball	EY01263
CG5912	arrow	EY04453
CG8909		GE5012
CG1372	yolkless	GE5203
CG12139		GE3293
CG33087		GS12223
		GE16005
CG5634	distracted	GS11284
		EY05482
		EP3400
CG32092		GE29338
		EY11189
		f02558
CG6863	Tolkin	GS69
CG32699		GS1129
		EP0352
CG7179		GS13316
		GS20243
CG32635		GE2396
CG3095		f06503
CG3413	windpipe	GE13015
CG3408		GS10831
CG4054		GE10226
CG5096		GS2165
CG5195		GS20382
CG5407	SUR-8	GS3141
CG5528	Toll-9	GS51
CG5810		f01959
CG5820	gp150	GS66
		EY08250
CG5851	sds22	f01874
CG6590		EY07744
CG6860		GE15908

CG6959		GE22610
CG7250	Toll-6	GE26496
CG7702		EY00368
CG8595	Toll-7	GE15025
CG8561	Acid labile subunit	GS10548
		GE12785
CG8896	18-wheeler	GS13286
		GE14005
CG9031		GS11003
CG9044		GS10919
CG10255	Lap1	GE10296
CG11280	tartan	GS10885
CG11282	capricious	GS10839
CG13125		GS11753
CG31137	twin	EY02330
CG31635		GS10303
CG14185		GE24319
CG14351		EY11244
CG14662		GE21218
CG14995		GS3174
CG15151	Pray for elves	GS11387
CG1504		GE4771
CG5784	Mapmodulin	EY01282
CG17335	Small bristles	GE4725
CG32687		GE2673
CG12002	peroxidasin	GS9354
CG12199	kekkon-like	GE3339
CG4192	kekkon 3	GS12192
CG12283	kekkon 1	GS7501
		EP655
CG9431	kekkon-4	GS10427
CG16974		EY01543
CG1804		GE28037
CG4096		GE5158
CG10145	M-Spondin	GS12735

CG10663		GS7321
		GE28907
CG17739		EY18336
CG31619		GS10109
CG7147	kuzbanian	GS11029
CG5661	Sema-5c	GS12797
CG18405	Sema-1a	GS2268
CG9095		GS8168
CG9138	SP1070	GS11655
CG1500	Furrowed	GS7008
CG2040	hig	GS10464
		EY03336
CG32146	dally-like	GS10784
CG2264	testican homolog	GE11359
		EY00918
CG3599	vanin homolog	GE2207
CG15671	crossveinless 2	EP1103
CG15828		G7994
CG14162	Dpr-6	f07173
CG31814		GS 10783
CG32791		GE2966
CG5803	Fasciclin 3	d05288
CG10972	ppk12	EY13952
CG31605	Bsg	GS11859
		EY10523
CG15138	Beat-IIIc	GS9617
CG10152	Beat-IV	EP3281
CG8434	lambik	GS17119
CG3903	gliotactin	GE13413
CG13349		GE14555
CG6789		GE5916
CG7052	Tep2	G3592
CG7068	Tep3	G2778
CG7586	Mcr	G3618
CG13079		GS11623

CG8084		GS9498
CG8827	Ance	G3223
CG10142	Ance-5	G3082
CG7013		G15626
CG4531	argos	GS12984
		d00253
CG6588	fasciclin I	d07727
CG3359	midline fasciclin	G3944
CG5758		GS22939
CG4280	croquemort	G3220
CG1887		f07156
CG2736		f02107
CG7000		GS10889
CG7228	peste	G3611
CG10345		f07636
CG4835		GS14786
CG5756		f07526
CG14796		G17286
CG2989		GE555
CG8756		GE17285
CG32209		d03931
CG17905		GE14153
CG32499		GE11981
CG4778		GE11195
CG10287	gasp	d02290
CG13312		GE29326
CG11372	Galectin	GS13007
		d09394
CG11374		GS11190
CG14879		G5507
CG32226		G4525
CG6895	GNBP1	G5241
CG5008	GNBP3	GS12348
CG6822		EP3212
CG6014		G15936

CG15765		G17073
CG9488	Discoidin domain receptor	f08070 d06926
CG6217		GS13403
CG12492		G13871
CG8399		G13327
CG32922		GS21977
CG7352		G4576
CG12004		GS16151 EY09136
CG5850		GS21004
CG13492		GS17711
CG10650		GS21331
CG7851		GS17574
CG33038		GE11809
CG15110	brother of tout-velu	GE15507
CG13194	pyramus	GS22603
CG12443	thisbe	G19748
CG8642		GS13795
CG17579	scabrous	GS9930
CG2507	stranded at second	GE24911
CG30418	nord	GS11012
CG9559	Fog	f06104 f05336
CG18734	Fur2	GE1121
CG10772	Fur1	EP3499
CG17697	fz	d04176 d04570
CG16785	fz3	GE1592
CG4626	fz4	GE31942
CG1106		GS10156
CG6575	gliolectin	EP3449
CG4934	brainiac	G68
CG8668		G2829
CG11357		G9588

CG3038		G728;-36
CG8673		EY15808
CG13904		GS11028
CG8734		GS6135
CG9520		G18317
CG10580	fringe	G5151
CG9659	egghead	G669
CG32540	CCKLR-17D3	GS22193
CG13702	allatostatin C receptor 2	d08685
CG33344	CcapR	f01987
CG10483		GE22810
CG10823		GS11212
CG12290		EY05347
CG12370		GE10659
CG13758		EY11851
CG13995		GS10590
		EP2273
CG18314		d05515
CG2061		EP1537
CG2901		GE3026
CG30106		f06893
		f06894
CG32843		f06589
CG4313		GE3444
CG4322		GE144
CG6919		f02819
CG6986		d00672
CG7431		d00913
CG7497		GE20576
CG8795		f02573
CG9643		EY07345
		f02198
CG8639	Cirl	GE12466
CG9569	DD2R	f06521

CG5911	ETHR	GE28632
CG6936	methuselah	d05374
CG17061	methuselah-like 10	GS21073
CG17795	methuselah-like 2	GS20687
CG6530	methuselah-like 3	GE15782
CG7476	methuselah-like 7	GS21256
CG8095	scab, volado	EP2591
CG5372		GS12413
CG1762	beta neu integrin	GE16247
CG32659	Tenascin accessory	GE1914
CG7466		GE10936
CG1077		GE27843
CG5392		EY01996
CG32354		GE24651
CG33466	follistatin	GE16028
CG31092	LpR2	GE24420
CG12497		GE5356
CG6739		d09967
CG1632		GE2039
CG32432		GE21767
CG4604	Glial Lazarillo	GE14060
CG9342		G3187
		d07488
CG1399		GS9001
CG8197		G7845
CG4168		f06058
CG12214		GE23737
CG14485	swi2	EY03082
CG17667		EY09216
CG2247		GE8222
CG7665	Fsh-Tsh-like receptor	GS16857
CG10702		GE17408
CG3837		GE22018

CG32464	l(3)82Fd	GS16948
CG1794		GS6122
CG9655	nessy	GS14209
CG9526		EY06644
CG17937	midway	EY07280
CG11495	rasp	GE21385
CG1221		G5226
CG18321		GE30385
CG11937	amnesiac	EP1571
		EP346
CG13633	Allatostatin	GE25324
CG18090	Drosulfakinin	GE26995
CG2346	FMRFamide-related	GS20864
CG13480	Leucokinin	f06006
CG3441	Neuropeptide-like precursor 1	GE16505
CG13061	Neuropeptide-like precursor 3	GS10896
CG13968	short neuropeptide F precursor	GE14853
CG7291	Niemann-Pick C2	GE12107
CG10183		EY02921
CG14204		G17581
		EY05761
CG11353		G4385
CG14205		G17121
CG13325		G19628
CG14219		G1281
CG32645		G488
CG5993		G17133
CG34378	Pvf3	f04177
CG13101		GS16273
		EY01250
		EP2168

CG9552	rolling stone	EP2569
CG9555		GE14634
		EY5571
CG4480		GS11125
CG12070	Saposin-related	d00213
		d00389
CG3376		XP d05970
CG15533		GS16402
CG10284		G4097
CG9540		GS22570
CG32679		G463
CG17210		GS16981
CG30486		GS13562
CG11977		GS13530
CG3921		GE10632
CG10221		GS11870
CG4316		G8915
CG2105		GE13145
CG3074		GS10363
CG6134	spaetzle	d02405
CG13313		GS21998
CG13499		d11680
		d00934
CG14760		GE12448
CG15153		GE10882
CG14280		GE20853
CG17264		EY07056
CG30371		GS14738
CG8075	Van Gogh	f04290
CG9614	pipe	G4081
CG10234	Hs2ST	GS6068
CG9550		GS18034
CG7890		G608
CG33147		EY11923
CG32373		GS14433

CG9093	Tsp26A	GE12891
CG8666	Tsp39D	d01894
CG14468	Tsp42A	GE14991
CG18817	Tsp42Ea	EP2210
CG12846	Tsp42Ed	GE12729
CG10106	Tsp42Ee	f06294
CG12845	Tsp42Ef	GS16897
		EP2608
CG12143	Tsp42Ej	GE13532
CG12840	Tsp42El	GE11349
		EY08356
CG12839	Tsp42En	GS12672
CG12837	Tsp42Er	GS14758
CG4690	Tsp5D	GE4237
CG4999	Tsp66E	GE30517
CG5492	Tsp74F	GE22775
CG4591	Tsp86D	GS12387
CG6120	Tsp96F	GE28078
CG16987	dawdle, Alp23B	G3085
CG5562	gbb	GS12725
CG8224	baboon	GS21092
CG7904	punt	GS22331
CG8647		GE27366
CG12410	crossveinless	G17312
CG11582		GS11766
CG18402	insulin-like receptor	f03155
CG4007	Nrk	GS8003
CG17559	dnt	GE10367
CG3915	drl2	f00086
CG31127	Wsck	GS16114
CG7103		G818
CG13780		G18227
CG3125		G282
CG13252		G5112
CG32647		d05563

CG1916	Wnt 2	d03132
		f00794
CG8804	wunen	GE20037
CG8805	wunen2	GS10006
		EP2527
CG11437		GE24251
CG11438		GS14810
CG12746		EY10535
CG13432		G11849
CG9355	dusky	G17259
CG15013	dusky-like	GS20894
CG15020		G19813
CG2467		G1385
CG10005		G4867
CG9369	miniature	EP0406
CG5847		G8605
CG1499		GE21553
CG7802		d07781
CG17111		f00307
CG17131	SP71	GE50193

This table lists the 311 genes screened in this paper and the corresponding insertion numbers. Additional information on all of these genes, including domain types and insertion positions, is included in Supplementary Table 1 of (Kurusu et al., 2008). For the screen in this paper, we removed genes from the Kurusu et al. list that seemed unlikely to encode ligands or coreceptors for CAM-like cell surface proteins. These included GPCRs, tetraspanins, neuropeptides, and others.

Supplemental References

Fashena, S.J., and Zinn, K. (1997). Transmembrane glycoprotein gp150 is a substrate for receptor tyrosine phosphatase DPTP10D in Drosophila cells. Molecular and cellular biology *17*, 6859-6867.
Iwaki, T., Figuera, M., Ploplis, V.A., and Castellino, F.J. (2003). Rapid selection of Drosophila S2 cells with the puromycin resistance gene. Biotechniques *35*, 482-484, 486.
Kurusu, M., Cording, A., Taniguchi, M., Menon, K., Suzuki, E., and Zinn, K. (2008). A screen of cell-surface molecules identifies leucine-rich repeat proteins as key mediators of synaptic target selection. Neuron *59*, 972-985.
Siebert, M., Banovic, D., Goellner, B., and Aberle, H. (2009). Drosophila motor axons recognize and follow a Sidestep-labeled substrate pathway to reach their target fields. Genes & development *23*, 1052-1062.